ISSN 1819-7140, Russian Journal of Pacific Geology, 2023, Vol. 17, No. 3, pp. 197–211. © Pleiades Publishing, Ltd., 2023.
Russian Text © The Author(s), 2023, published in Tikhookeanskaya Geologiya, 2023, Vol. 42, No. 3, pp. 3–19.

The Structure of the Earth's Crust and Lithospheric Mantle in the Central Part of the Lower Amur Metallogenic Zone and the Gold Distribution within It

M. Yu. Nosyrev[a, *], A. N. Didenko[a, b], and G. Z. Gil'manova[a]

[a] *Kosygin Institute of Tectonics and Geophysics, Far Eastern Branch, Russian Academy of Sciences, Khabarovsk, 680000 Russia*
[b] *Geological Institute, Russian Academy of Sciences, Moscow, 119017 Russia*
**e-mail: ns041ck@yandex.ru*

Received November 28, 2022; revised December 28, 2022; accepted January 23, 2023

Abstract—In this study, we consider the deep structure of the Earth's crust and the lithospheric mantle in the central part of the Lower Amur metallogenic zone and its western flank, which includes the Albazino gold ore cluster. Zones with a sharp change in density and magnetic properties associated with Late Cretaceous–Early Paleogene magmatism were established based on the calculated density and magnetic depth models of the territory. A ring structure ~200 km across was identified, which is characterized by the low-density lithospheric mantle and density and magnetic inhomogeneities in the Earth's crust, which are related with a wide development of intrusive bodies within it, as well as their spatial position and composition. The spatial relation of gold ore districts, clusters, and deposits to the density and magnetic inhomogeneities in the crust and lithospheric mantle has been analyzed and the main patterns in their distribution are shown. As a rule, they are confined to the low-density zones in the crust and marginal areas of deep-seated (12–20 km) magnetic intrusions. Based on the conclusions, new promising areas to prospect for gold deposits are proposed. In particular, it was concluded that the potential of the western part of the ring structure to the south of the Albazino deposit to host gold mineralization was underestimated.

Keywords: magnetic and density depth models, promising areas to prospect for gold deposits, ring structurem Pilda–Limuri gold ore district, Russian Far East

DOI: 10.1134/S1819714023030077

INTRODUCTION

The Lower Amur metallogenic zone [4] is located within the northern part of the Sikhote-Alin orogenic belt and extended for 550 km in the northeastern direction from Lake Bolon' in the south to the Sea of Okhotsk coast in the north. The main mineral resource of the zone is gold. The zone can be subdivided into three areas: (1) the northern area including the large Mnogovershinnoe epithermal deposit and several occurrences of similar genesis; (2) the southern weakly studied area with high prospects for the copper porphyry and gold mineralization (the world-class gold–copper–porphyry deposit was discovered in this area 15 years ago); and (3) the central area with abundant bedrock deposits, which are united into the Pilda–Limuri and Kherpuchin gold districts, which are the historical center of gold mining in the region.

The deposits of the central area are mainly small and subeconomic. However, the recent discovery of the high-grade Chulbatkan deposit and successful prospecting of the Dyappe deposits, as well as the proximity of the Albazino ore cluster with its eponymous large deposit highlight need a revision of the gold potential of this territory. One of the most important tasks of this study is to determine the relationship between the distribution of mineralized objects and physical inhomogeneities in the Earth's crust and lithospheric mantle, to develop the depth structural models and to provide their geodynamic and genetic interpretation.

Practically all deposits of the zone have a clear spatial relationship with the Late Cretaceous magmatic rocks, which are mainly represented by small stocks and dikes of intrusive rocks and by the relatively large Chulbatkan intrusion at the Chulbatkan deposit. Genetically, the formation of these deposits is also thought to be related to the Late Cretaceous magmatism. The tight relationship of gold mineralization of the considered area with the Late Cretaceous magmatism shows an important role of geophysical data in studying the deep position of magmatic bodies and signs of magmatic processes in the Earth's crust and mantle. The depth structure of the central part of the Lower Amur metallogenic zone and its western flank containing the Albazino gold deposit was studied

based on the gravitational and anomalous magnetic fields and creation of the depth prediction model (Fig. 1).

GEOLOGICAL CHARACTERISTICS AND ORE POTENTIAL

The considered area is located at the juncture of several terranes made up of Jurassic and Cretaceous sedimentary rocks, which are ascribed to the Sikhote-Alin (Zhuravlevka–Amur and Badzhal terranes) and Mongol–Okhotsk (Ulban terrane) orogenic belts [26] (Fig. 1). In the paleogeodynamic aspect, this area represents a fragment of Late Cretaceous continental margin [3], evolution of which determined the deep structure of this territory. A simplified geological map of the area compiled using geological maps at a scale of 1 : 1000000 [6, 8, 10, 12] is shown in Fig. 1.

This area is mainly made up of Jurassic–Cretaceous sedimentary and, less commonly, volcanogenic rocks. Early Cretaceous turbidite deposits (Gorinskaya, Pionerskaya, and Pivanskaya formations) mainly represented by alternation of siltstones and sandstones in variable proportions are developed in the eastern part of the Zhuravlevka–Amur terrane. Small areas are occupied by the Gornaya Protoka Formation of varying compositions from sandstones to gravelstones. Deposits of the Silasin Formation (siltstones, sandstones, their tuff varieties) occur in the southeastern part of the area.

The western part is made up of Jurassic sediments ascribed to the Ulbin, Mikhalitsinskaya, Elgon, Silinskaya, and Padalka formations. These are mainly sandstones and siltstones, with scarce intercalations of siliceous rocks and sometimes basalts. Late Carboniferous (Berenda and Krestovskaya formations) and Triassic deposits are exposed in a small tectonic block in the west. There are also spacious fields of volcanogenic rocks ascribed to the Omeldinsky and Maloomeldinsky complexes of Late Cretaceous age. The former is represented by lavas and tuffs of andesites, basaltic andesites, and more rarely dacites. The rocks of the Maloomeldinsky Complex in general have felsic compositions: dacites, rhyodacites, andesites, and their tuffs. Both the complexes contain subvolcanic intrusions, which are united into the Evur volcanoplutonic area. It includes several volcanotectonic structures, the largest of which, the Evur structure, is 40 × 60 km in size. Several volcanogenic edifices of the smaller size (Kharpi, Verkhnii Boktor, Ol'kogol) are known to the south of it. The formation of the Evur Complex developed within the eponymous volcanoplutonic area likely occurred in two or four phases in the first half of the Late Cretaceous [11, 19].

The youngest rocks are Miocene basalts, basaltic andesites, trachybasaltic andesites, and trachynadesites of the Ayakit sequence of the Ayakit volcanogenic complex. In the western part of the area, they fill near-valley areas of the Evur, Bichi, and Kharpichikan rivers.

The studied territory comprises abundant Late Cretaceous intrusive rocks. They are united into three intrusive complexes: Lower Amur, Evur, and Ul'ban [7, 9, 11, 13]. The eastern part of the area is dominated by the intrusive rocks of the Lower Amur Complex, while the rocks of the Evur and Ul'ban complexes are developed in the western part. Magmatic rocks form both large massifs and series of small equant bodies and dikes. All three complexes are multiphase. The first phase produced gabbrodiorites and diorites, while the second, main, phase is mainly represented by granodiorites, and the rocks of the third, final phase, are close to granites. The latter form small intrusions (up to 5 km^2 in area) and out-of-scale fracture bodies, which usually lie among the rocks of the marginal zones of large massifs of the second phase. All intrusive massifs are surrounded by the wide contact aureoles represented mainly by hornfels. The central part of the area contains two Paleocene granitoid massifs ascribed to the Bekchiul Complex. The textural–structural features and inner zoning of the Paleocene

Fig. 1. The terrane scheme of the Sikhote-Alin orogenic belt and position of the studied area (a) after [3, 26], and simplified geological map of the studied area (b) after [6, 8, 10, 12]. (a): (*1*) Precambrian ((SB) Siberian Craton (a)) and Early Paleozoic superterranes ((b) (BR) Bureya, (JS) Jiamusi, (KH) Khanka); (*2*) fragment of terrane of the Early Paleozoic continental margins ((SR) Sergeevsky); (*3*) terranes of the Permotriassic accretionary wedge ((DK) Dzhagdy-Kerba, (NL) Nilan, (LG) Laoeling-Grodekovo); (*4*) terranes of the Jurassic turbidite basins ((UL) Ulban and Un'ya-Bom); (*5*) terranes of the Jurassic accretionary wedge ((SM) Samarka, (ND) Nidankhada–Bikin, (KHB) Khabarovsk, (BD) Badzhal); (*6*) terranes of the Hauterivian–Albian accretionary wedge ((TU) Taukhe); (*7*) Early Cretaceous turbidite basins ((ZHA) Zhuravlevka–Amur); (*8*) terranes of the Early Cretaceous island arc (KM) Kema, (UD) Uda); (*9*) terranes of the Early Cretaceous accretionary wedge ((KS) Kiselevka–Manoma); (*10*) contour of the studied area; (*11*) boundary of the Lower Amur metallogenic zone after [4] ((1) Albazino gold cluster, (*12*) Pilda–Limuri gold district, (3) Kherpuchin gold district). (b): (*1*) undivided Quaternary deposits; (*2*) Neogene basalts, basaltic andesites (Ayakit volcanic complex); (*3*) Upper Cretaceous volcanogenic rocks, andesites, dacites (Omeldinsky volcanic complex), dacites, rhyolites (Maloomeldinsky volcanic complex), their extrusive and subvolcanic analogues (including separate volcanic structures: (a) Evur, (b) Kharpi, (c) Verkhnii Boktor, (d) Ol'gokol); (*4*) Upper Cretaceous sedimentary rocks (Gorinskaya, Ponerskaya, Pivanskaya, Gornoprotoksyaa formations); (*5*) Upper Jurassic sedimentary rocks (Padalinskaya, Silinskaya formations); (*6*) Lower–Middle Jurassic sedimentary rocks (Mikhalitsinskaya, Ulbinskaya, El'gonskaya formations); (*7*) Upper Carboniferous sedimentary rocks (Krestovaya, Berenda formations); (*8*) Late Cretaceous subvolcanic rhyolites, trachyrhyolites; (*9*) Early Paleogene granites (Bekchiul intrusive complex); (*10*) Late Cretaceous intrusions: granodiorites, diorites, and granites (Lower Amur, Evur intrusive complexes); (*11*) main faults; (*12*) bedrock gold deposits: (1) Albazino, (2) Chulbatkan; (3) Oktyabr'skoe, (4) Pokrovo-Troitskoe, (5) Agnie-Afanas'evskoe, (6) Dyappe, (7) Martem'yanovskoe, (8) Uchaminskoe, (9) Delken; (13) bedrock gold occurrences; (14) gold mineralization spots.

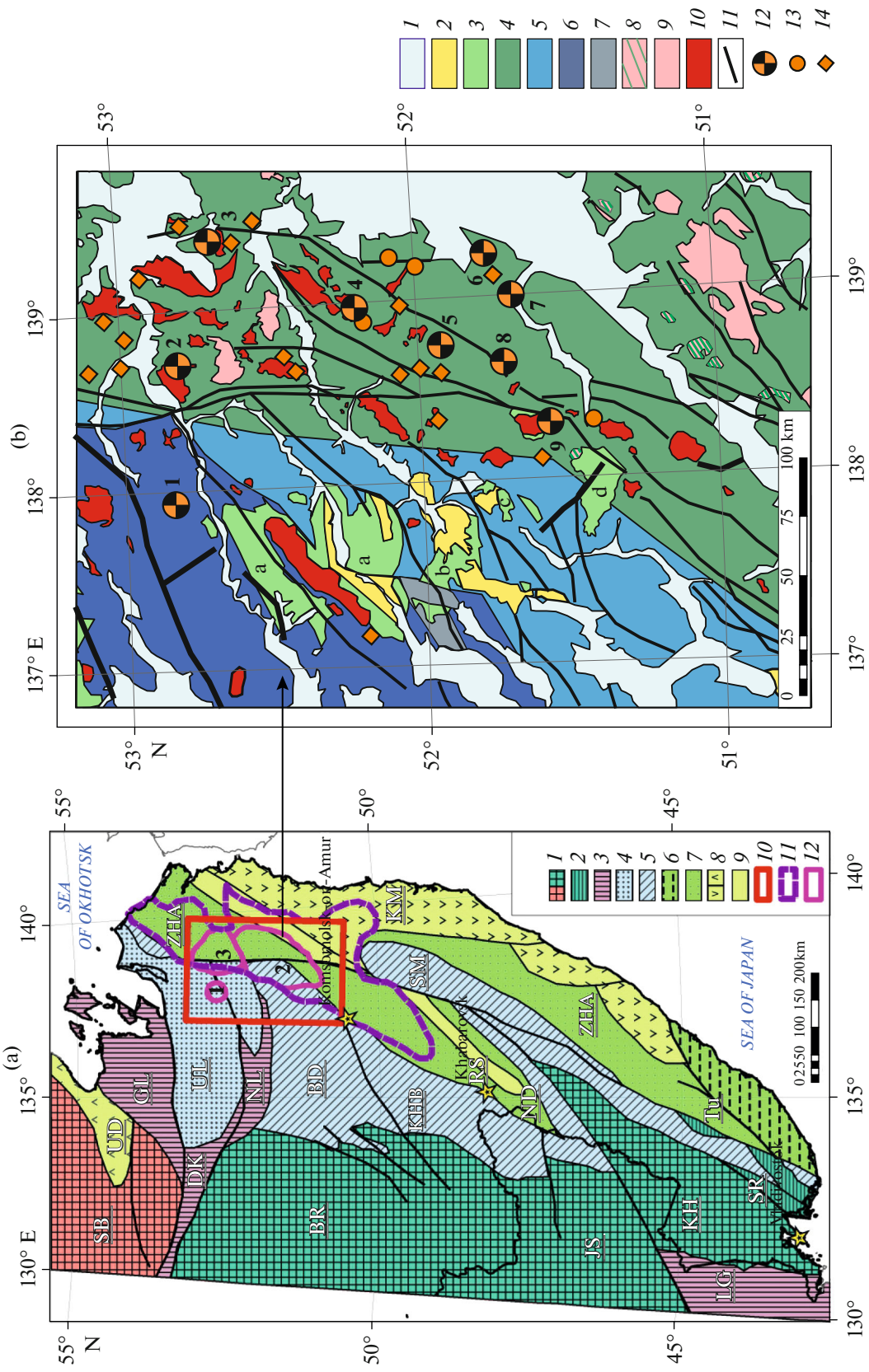
(a)
(b)
SEA OF OKHOTSK
SEA OF JAPAN
Komsomol'sk-on-Amur
Khabarovsk
Vladivostok
SB
UD
GL
UL
DK
NL
BD
KHB
BR
JS
LG
KH
SR
ND
RS
SM
ZHA
KM
Tu
0 25 50 75 100 km
0 50 100 150 200km
130° E
135°
140°
55° N
50°
45°
137° E
138°
139°
53° N
52°
51°

massifs point to a shallow depth of their emplacement [11].

The area is intersected by a series of regional faults. It is divided roughly in half by the large NS-trending Limurchan Fault, and the V'yunsky Fault of the same orientation is distinguished to the east. The NE-trending faults are also widespread [6, 8, 10, 12].

The main mineral resource of the area is gold. There are numerous bedrock gold deposits of different scales and degrees of study. The largest of them is the Albazino deposit, which was explored in 2007–2008 and at present is mined by JSC Polimetall. It is located within deeply eroded paleocaldera [24]. In the volcanic structure, the terrigenous rocks of the basement are intruded by numerous dikes and stocks of mainly moderately felsic composition. The intrusive bodies are mainly small (up to 4–5 km^2), belong to the subvolcanic facies, and have laccolithic or lopolithic morphologies. Ore zones are restricted to the extensional NS- and NW-trending fault structures. The highest gold concentrations were found in the central part of beresitization aureole with linear stockworks of quartz and quartz–carbonate veinlets with sulfide mineralization. The ores contain 2–6% sulfides. Mineralization occurs both in sandstones and in granodiorite dikes. According to [24], the gold mineralization can be ascribed to the gold–sulfide–quartz formation, gold–low sulfide mineral type. The deposit was formed in the Late Cretaceous and is genetically related to the final stage of magmatic activity. According to the cited authors, the ore-generating paleomagmatic chamber (Brusnichnoe subvolcanic body) is distinguished in the central part of the caldera. Thus, the rocks of the entire caldera were highly fractured and subjected to the hydrothermal reworking. In general, the formation of large gold deposit is determined not only by the structural–lithological factors, but also by the presence of the Lower Amur granodiorites specialized for gold.

In recent years, the large Chulbatkan gold deposit was discovered in the northern part of the considered area, in the Amgun River valley. It is located in the shear zone at the contact of the Chulbat plagiogranite massif and hornfelsed sandstones and siltstones of the Gorinskaya and Pionerskaya formations, being controlled by the subsidiary ENE-extending faults of the main NE-trending fault [1]. The deposit is represented by a system of steeply dipping mineralized zones. Most of them occur in the intrusion and only scarce thin bodies on the northeastern flank are localized in the hornfelsed terrigenous rocks. Hydrothermal alterations are represented by beresites overprinted by later silicification and abundant latest carbonatization. The only useful component in the ore is gold. The deposit is ascribed to the poor sulfide quartz–gold formation.

The eastern part of the area comprises several small gold deposits: the Agnie-Afanas'evskoe, Pokrovo-Troitskoe, Oktyabr'skoe, Dyappe, Martem'yanovskoe, Uchaminskoe, and Delken ones. There are also many occurrences of similar types (Fig. 1). These deposits have been described in detail in many papers and monographs [21] and will not be considered below. All of them, except for the Uchaminsky deposit, belong to the gold–quartz formation. The Uchaminsky deposit can be regarded as an object of gold sulfide formation.

Several important facts can be drawn from the above considered literature data on the geology and gold potential of the region.

(1) The known gold deposits are localized both in the Early Cretaceous and Jurassic sedimentary rocks (Albazino and Delken).

(2) All the deposits show a clear spatial ship with Late Cretaceous magmatic rocks. Gold fields contain small intrusive stocks and dikes of intrusive rocks, while the Chulbatkan deposit contains the relatively large Chulbat intrusion. Genetically, these deposits are also thought to be related to the Late Cretaceous magmatism.

(3) Gold mineralization is localized both in sedimentary rocks, including honfelsed (most part except for the Chulbatkan deposit)deposits, and in the magmatic complexes: dikes, stocks, and larger intrusive massifs.

(4) Mineralization at all deposits reveal distinct structural control, being confined to the faults of different orientation.

(5) Although gold mineralization is mainly ascribed to the gold–quartz or sulfide gold–quartz types at extremely low content of sulfide minerals, some objects are characterized by the abundant sulfide mineralization (Uchaminsky deposit and some occurrences).

A tight relationship of gold mineralization of the considered area with Late Cretaceous magmatism once more emphasizes the importance of geophysical data for the determination of depth position of intrusive bodies, signs of magmatic processes, and fluid saturation of the Earth's crust and mantle.

INITIAL MATERIALS AND METHODS OF THEIR PROCESSING

During our works, the gravitational and magnetic anomalous fields of the territory were analyzed to develop a 3D model. Initial materials were digital models of the gravity and magnetic fields obtained when creating the digital geophysical basis for the State Geological Map on a scale 1 : 1000000. Thus, the digital model of the gravity field was based on the gravimetric survey on a scale 1 : 200000, which covered practically the entire studied area. This allowed us to obtain working grid with a 1-km cell size. The model of anomalous magnetic field is based on the results of airborne geophysical survey on 1 : 50000–

1 : 200000 scales, which provided the 0.5 km cell size of working grid.

The 3D models of density and magnetic parameters were constructed using the COSCAD-3D software package [20, 23]. The "Statistical Assessment of Parameters of Anomaly-Forming Objects" applied algorithm is based on the known variation method [2], which was additionally modified by authors of the software. The density model was calculated from the Bouguer gravity up to 60 km. The reduced-to-pole magnetic model was calculated for the magnetic field to a depth of 20 km, because the thickness of the magnetically active layer at the studied area is, on average, 20 km [19]. As a result, we obtained a 3D model of the distribution of the effective density and magnetization in arbitrary units over 1 × 1 × 1 km grid for density and 500 × 500 × 500 m grid for magnetic models. The deeper lithospheric horizons were characterized using density model previously calculated by authors for the entire Sikhote-Alin orogenic belt up to a depth of 130 km [15]

ANALYSIS OF DEPTH MODELS AND THEIR INTERPRETATION

Magnetic Model

The anomalous magnetic field of the studied area and horizontal sections over several depth levels of the magnetic model are shown in Fig. 2. Based on the initial magnetic field and depth modeling, a ring structure (RS) is distinguished at the considered territory practically over the entire thickness of magnetically active layer. It spans series of magnetic bodies that are localized at different depths, alternating with zones of nonmagnetic rocks. The external size of the RS is ~150 × 190 km and the large axis has a sublongitudinal direction. The RS, in turn, also has a zoned structure. It contains central core ~80 × 90 km in size, which compared to the peripheral region is characterized by the significant decrease of number of magnetic bodies in the Earth's crust, especially starting from a depth of 10 km (Fig. 2).

As follows from the model, the magnetic bodies are distributed over three levels. The lowest level (>12 km) contains large magnetic bodies with high effective magnetization, which are confined to the peripheral part of the RS, beyond its central part. These are mainly equant or weakly extended bodies 10–25 km across. In the eastern part of the RS, they are confined to the arc-shaped external segment. In the western part, they are arranged as sublongitudinal band (Fig. 2d), being likely restricted to the inferred deep-seated faults of such orientation. These magnetic fields are interpreted as deep roots of magnetic intrusions.

The magnetic bodies of the middle level (4–8 km) are characterized in general by lower effective magnetization and have smaller sizes compared to the bodies of the previous level. These are likely separate intrusive bodies. In plan, they are conjugate with magnetic bodies of the lowermost level, but are frequently shifted from root parts of the intrusions. Trans-magnetic bodies that are traced uninterruptedly from the surface to a depth over 10 km are rare. Sometimes, this level is devoid of magnetic bodies corresponding to the lower level. Thus, they could appear at higher levels. Such a discontinuous structure of the magmatic column is explained by the presence of horizontal discontinuities in the crust, where the permeability of the section could change, which leads to the multilevel arrangement of magmatic chambers in the crust [16]. One more characteristic feature of magnetic bodies of this level is the well-expressed linearity in some cases, which suggests their confinement to the fault zones.

Third, the subsurface level of magnetic bodies spans mainly depths up to 1–1.5 km. Some of them correspond to the known intrusive massifs, while others are located in the vicinity and could be interpreted as unexposed portions of the intrusions. However, some magnetic bodies are not correlated with known massifs and likely represent unexposed intrusions. A complex system of magnetic bodies is typical of areas of volcanogenic rocks, where magnetic bodies could correspond both to the covers of basalts and andesites, and to the separate extrusive edifices and subvolcanic intrusions.

The main magnetic bodies of this level are correlated with deep anomalies of effective magnetization, but complete coincidence is not observed. For more detailed interpretation, this depth level should be studied by a large-scale magnetic survey during prospecting works within ore fields.

The Density Model

The gravity field map for the studied area and density distribution at different depths are shown in Fig. 3. It should be emphasized that the density distribution in the Earth's crust and mantle are spatially correlated to the ring structure distinguished based on the magnetic field, emphasizing and confirming it. This is especially clearly expressed at two depth levels: 8–20 km (middle crust) and >50 km (Fig. 4). Within the Earth's crust, the considered ring structure is characterized by a low-density periphery and a relatively high-density central block, which coincides with the central part distinguished based on the model magnetic data. These local low-density regions have equant or weakly extended shape, with size 15–35 km across. The local density decrease over periphery of the ring structure is interpreted as the regions of development of granitoid intrusions and the total decompaction related to the destruction and changes of the Earth's crust in the magma-permeable zones. The less detailed gravimetric data compared to data of magnetic survey makes it impossible to divide with confidence the low-density region by depths. Therefore, a single magma column is fixed. It should be also noted that these low-density

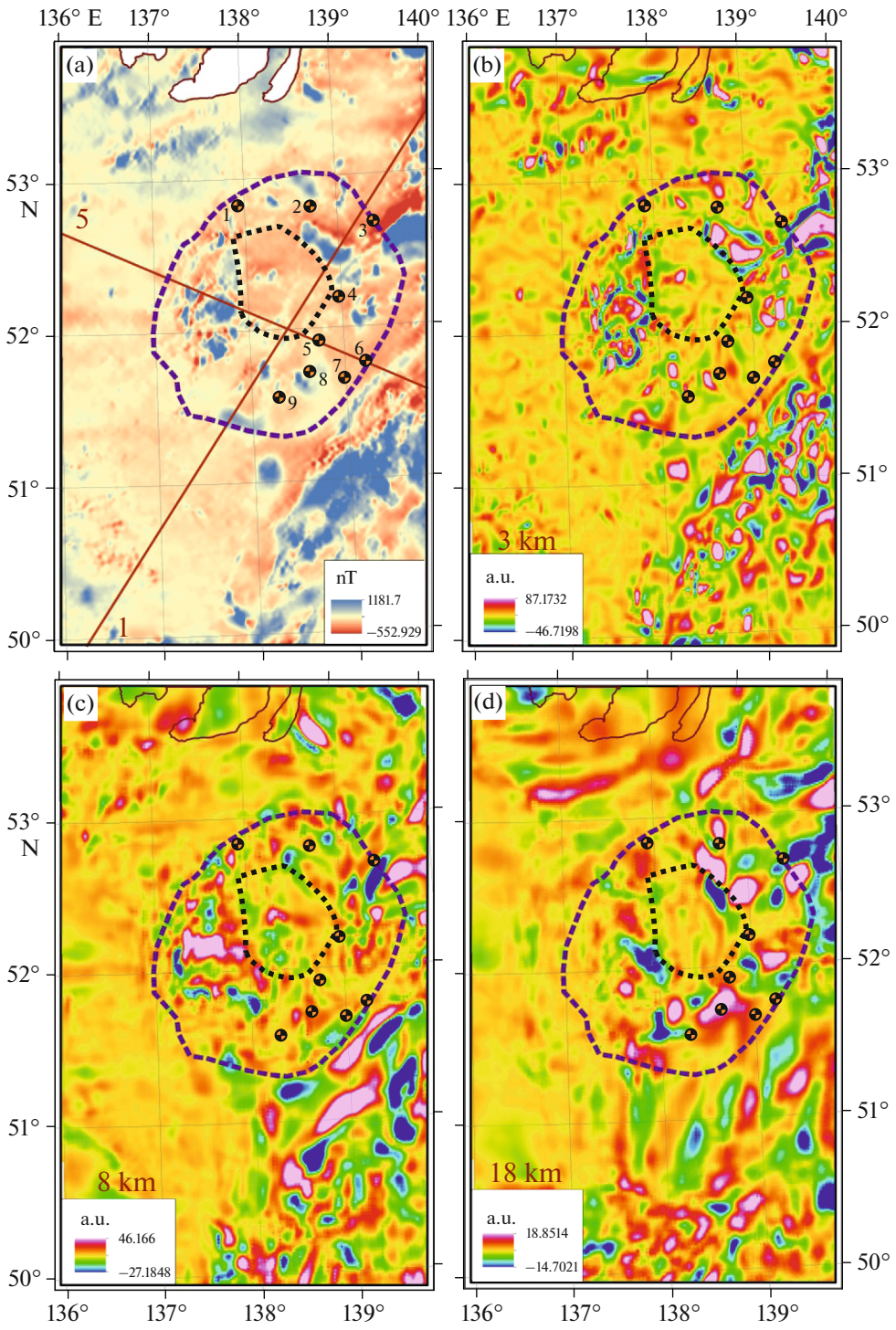

Fig. 2. A magnetic depth model of the central part of the Lower Amur metallogenic zone. (a) Map of anomalous magnetic field; (b–d) maps of effective magnetization at depths of 3, 8, and 18 km, respectively. Gauss-Kruger projection, central meridian 135°. Violet and black dashed lines show boundaries of ring structure and its central part (see text for explanation). Red straight lines 1 and 5 in Fig. a shows the position of calculated profiles of effective magnetization demonstrating in Fig. 4. Bedrock gold deposits: (1) Albazino, (2) Chulbatkan, (3) Oktyabr'skoe, (4) Pokrovo-Troitskoe, (5) Agnie-Afanas'evskoe, (6) Dyappe, (7) Martem'yanovskoe, (8) Uchaminskoe, (6) Delken.

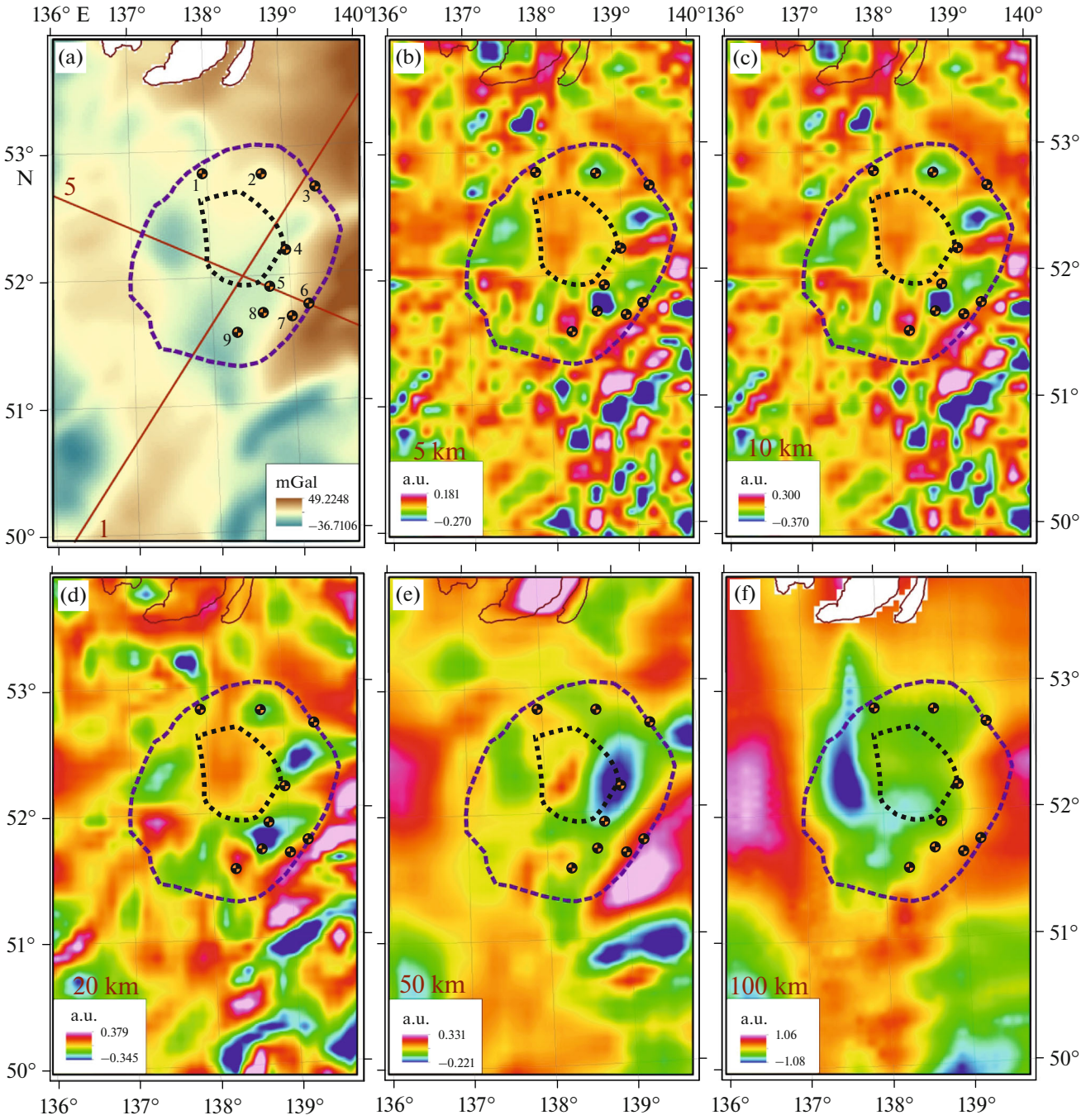

Fig. 3. A density depth model of the central part of the Lower Amur metallogenic zone. (a) Map of the Bouguer gravity; (b–f) map of effective density at depths of 5, 10, 20, 50, and 100 km, respectively. The Gauss–Kruger projection, central meridian 135°. Violet and black dashed lines show boundaries of the ring structure and its central parts (see text for description). Red lines 1 and 5 in "a" shows the position of calculated effective density profiles demonstrated in Fig. 4. Bedrock gold deposits: (1) Albazino, (2) Chulbatkan, ((3) Oktyabr'skoe, (4) Pokrovo-Troitskoe, (5) Agnie-Afanas'evskoe, (6) Dyappe, (7) Martem'yanovskoe, (8) Uchaminskoe, (6) Delken.

regions are developed both in the eastern and western parts of the structure. The low-density zones at depths of 10–20 km are spatially conjugate with magnetic bodies of this level; however complete coincidence is absent and magnetic bodies more frequently occupy marginal parts of the low-density areas. All this indicates that multiphase granodiorite and granite intrusions occupy the most part of the structure, thus determining the presence of negative gravity anomalies and the low-density areas in the Earth's crust. It is also possible that large granite massifs are hidden at depth. Only in one case, part of the zone of extremely high

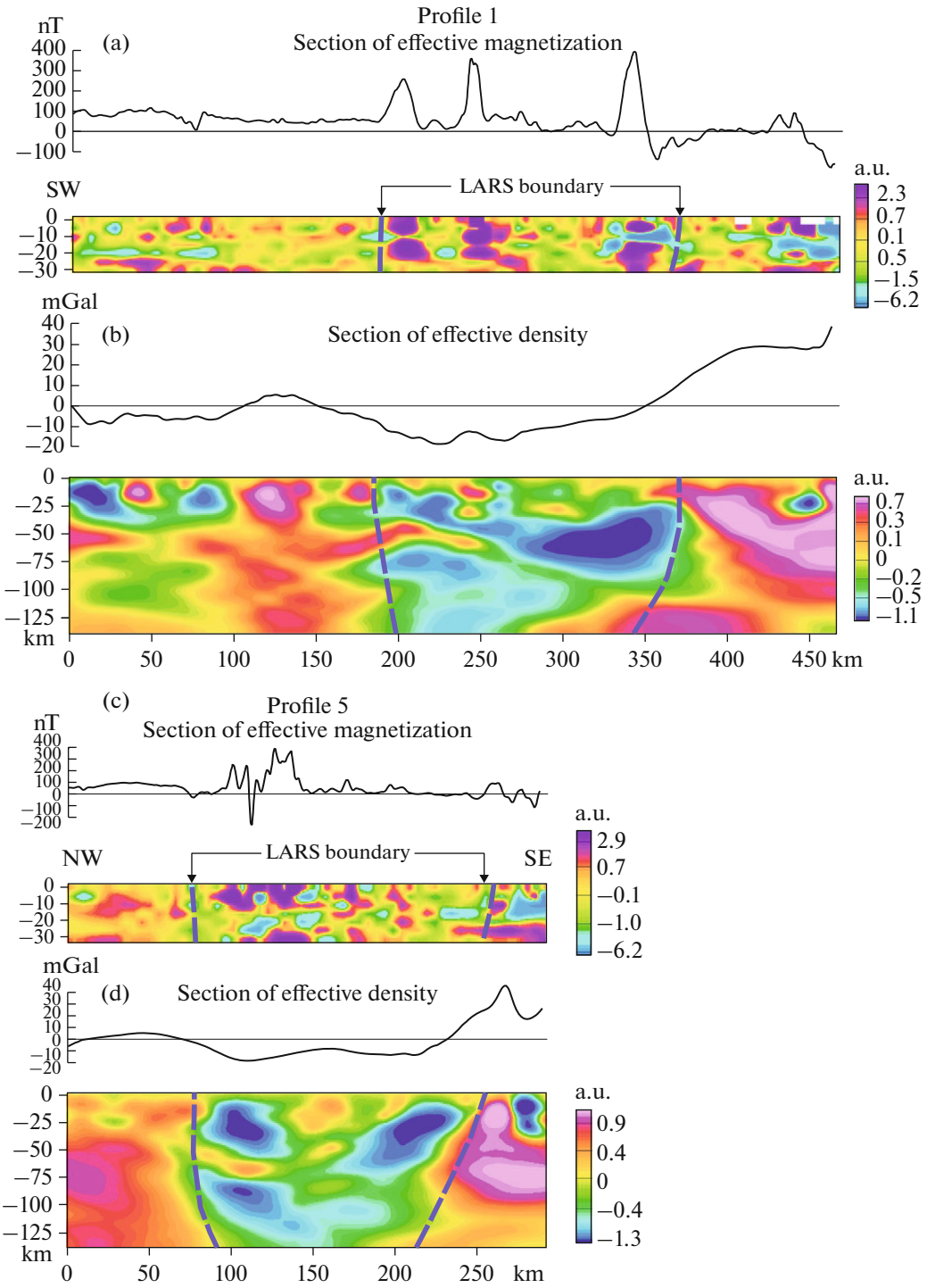

Fig. 4. The depth profiles of effective magnetization and effective density. Profile 1: (a) section of effective magnetization with plot of anomalous magnetic field; (b) section of effective density with plot of the Bouguer gravity; profile 5: (c) section of effective magnetization with plot of anomalous magnetic field. (d) section of effective density with plot of the Bouguer gravity.

effective magnetization at a depth of 14–20 km coincides with the center of the low-density area. This is observed in the area of the Uchaminsky gold deposit, but even in this case the western half of the effective magnetization anomaly is located in the marginal part of the low-density zone.

In addition to the central high-density block, the extremely high-density area is distinguished based on

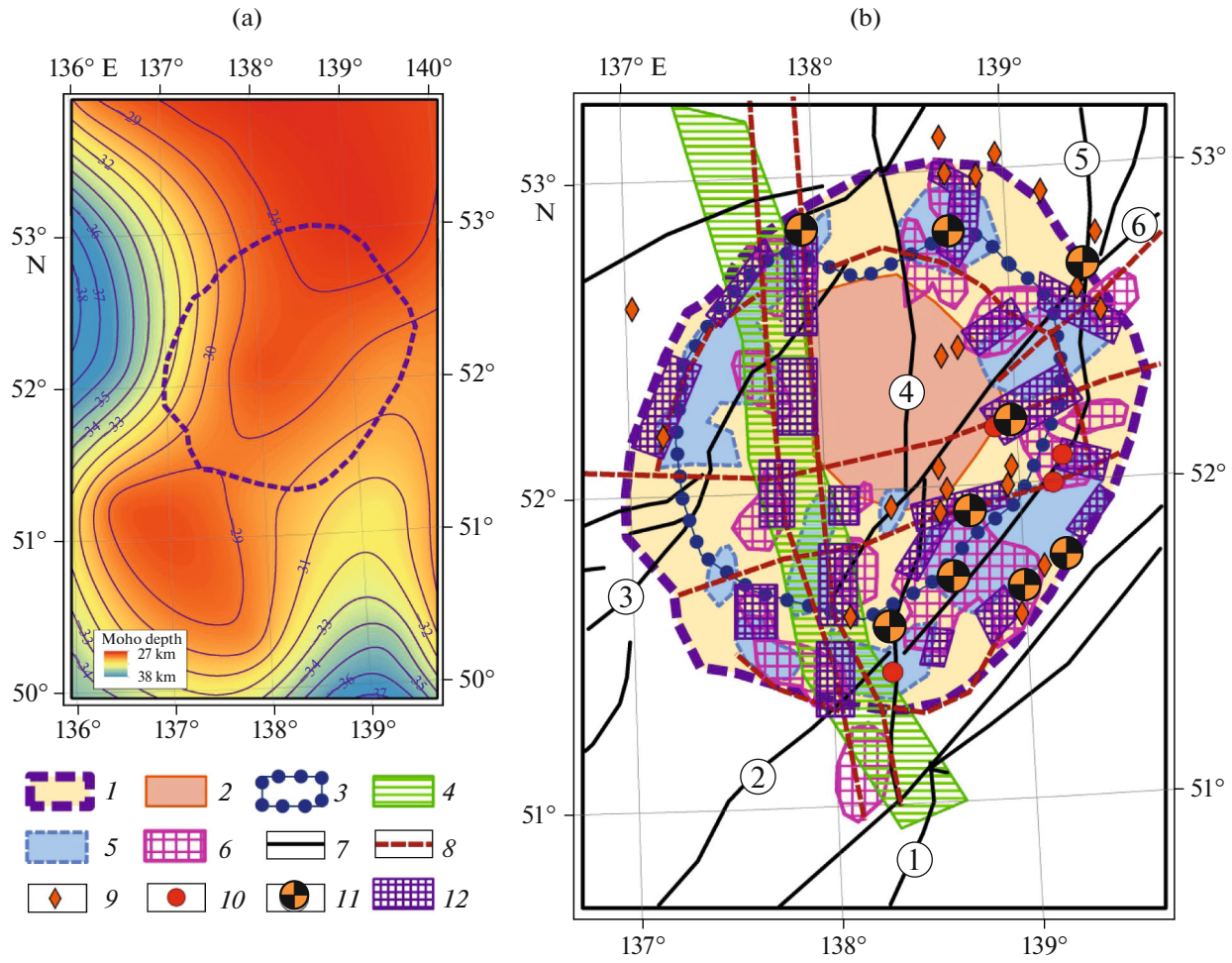

Fig. 5. A geological feological–geophysical depth model of the Limuri–Amgun ring structure and promising areas for gold deposits. (a) Projection of outline of the Limuri–Amgun ring structure on the Moho projection [25]; (b) scheme of depth structure of the Limuri–Amgun ring structure and promising areas to prospect gold deposits. (b) (*1*) boundary of the Limuri–Amgun ring structure and its peripheral part; (*2*) inner "core" of the Limuri–Amgun ring structures; (*3*) outlines of the maximum decompaction area in the upper part of lithospheric mantle (50–80 km); (*4*) linear decompaction zone in the lower part of lithospheric mantle (120 km); (*5*) low-density areas in the upper and middle parts of the Earth's crust (up to 25 km); (*6*) outlines of magnetic bodies at depths of 14–20 km; (*7*) main faults after [18], including: (1) Central Sikhote Alin, (2) Boktorsky, (3) Dukinsky, (4) Limurchansky, (5) V'yunsky, (6) Bichi-Amursky; (*8*) faults distinguished based on geophysical data (this work); (*9*) gold mineralization, (*10*) gold occurrences; (*11*) Gold deposits: (1) Albazino, (2) Chulbatkan, ((3) Oktyabr'skoe, (4) Pokrovo–Troitskoe, (5) Agnie-Afanas'evskoe, (6) Dyappe, (7) Martem'yanovskoe, (8) Uchaminskoe, (6) Delken; (*12*) outlines of promising areas to prospect gold deposits.

gravimetric data within the outer zone in the southwestern part. This increase is related to the ledge of dense rocks of the Triassic accretionary wedge where Early Carboniferous rocks are saturated in basalts (up to 500-m thick in the Berenda Formation) [11].

From a depth of 40–50 km and up to the studied depth of 130 km, the ring structure is underlain by the well-expressed low-density area dipping to the west (Figs. 3e, 3f). Given that the lithosphere thickness in this area is 120–130 km [5], the revealed low-density area characterizes the upper mantle metasomatically reworked by ascending fluids and melts in subduction mantle wedge and by formation of magma chambers at different depths. Similar processes and corresponding physical inhomogeneities are sufficiently well studied in the modern subduction zones [17]. It is also seen that a single low-density mantle area at the crustal level is divided into several more local zones, "jets," which to different extents extend to the Earth's crust and determine the local low-density areas in the upper crust and the areas of development and concentrations of magmatic processes at different depth levels. The central relatively high-density core likely is less permeable for magmatic melts and fluids, which determined their lower impact on the crust, its lower decompaction, and the small amount of magmatic complexes.

The low-density mantle zone is inclined to the west and southwest, and its deepest part is located beneath the western half of the ring structure (Fig. 4). This deep low-density zone becomes linear, has a longitu-

dinal orientation and is traced in the northern direction beyond the considered ring. This band likely records the deepest permeable area in mantle. Peculiarities of the considered density inhomogeneities are also clearly seen in the sections (Fig. 4).

The considered geophysical data give grounds to distinguish within the studied area a definite zone of ring shape, which is characterized by peculiar deep characteristics. Further, this structure will be termed the Limuri–Amgun ring structure (LARS) after the rivers running on its southern and northern flanks. It should be noted that the distinguished structure spans both the central part of the Lower Amur metallogenic zone as well as the Albazino gold cluster in the western flank, and the territory already ascribed to the Amur metallogenic province [4].

Figure 5 shows the depth scheme of this structure, which demonstrates the main considered patterns.

Note also that the LARS and entire Lower Amur metallogenic zone occupy a definite position relative to the Moho discontinuity, being located above a narrow and extended area of reduced crustal thickness, above the mantle ledge, which is limited by the escarps reaching the highest amplitude in the west (Fig. 5). The Moho depth is taken from [25], where it was calculated based on the spectral analysis of the gravity field.

Geophysical materials also give information on the linear fault zones, which represent an important factor of gold localization. In this work, in addition to large faults known from geological data, we also show the main linear elements of physical fields and boundaries of the change of physical properties in the Earth's crust and lithospheric mantle, which could be interpreted as faults. The identification of these elements is of great importance, since they could control the localization of gold mineralization (Fig. 5).

The most important of them is a sublongitudinal fault passing in the western part of the ring structure through the Albazino deposit (Fig. 5). It is suggested that this could be the large fault (fault zone) that is parallel to the Limurchan Fault and spaced from it at a distance of 40–50 km to the west. This fault serves as the eastern boundary of the Evur volcanoplutonic area. A series of magnetic bodies, inferred intrusions, is confined to this fault at depths over 12 km. As mentioned previously, it limits the linear low-density zone at mantle level. Several sublongitudinal low-density zones are also distinguished in the crust beneath the separate volcanotectonic structures.

The considered RS has a magmatogenic origin and is characterized by relatively high (compared to the adjacent territories) concentrations of Late Cretaceous intrusions within its limits, as well as by the presence of fields of volcanogenic rocks. The low-density areas at depth are interpreted as intrusive centers, multiphase intrusive bodies, and permeable zones. Magnetic bodies correspond to the separate magnetic intrusions, but they show no complete coincidence with the low-density areas, which suggests a limited volume of magnetic phases in the total volume of magmatic bodies. The magnetic data also record separate shallow intrusions (3–5 km), which is very important for the assessment and prediction of gold potential of the territory.

Thus, the Limuri–Amgun ring structure distinguished from geophysical data in the central part of the Lower Amur metallogenic zone and its specific depth structure are caused by the intense magmatic processes and reworking of the crust and upper mantle at the Pacific Asian margin in the Late Cretaceous–Paleocene. A single magmatic process spanned terranes made up of both Cretaceous and Jurassic sediments. This stage was also responsible for the formation of gold deposits.

THE DISTRIBUTION PATTERN OF GOLD MINERALIZATION WITHIN THE LARS AND RECOGNITION OF PROMISING AREAS

As was shown above, the LARS includes many gold-bearing objects, most of which are confined to its eastern part. The western part is mainly composed of Jurassic sedimentary complexes and Upper Cretaceous volcanogenic rocks and has lower gold potential than the eastern part. This part contains only the Albazino deposit and several gold occurrences.

Metallogenic units comparable in size with the considered deep-seated inhomogeneities are gold bearing districts, clusters, fields, and separate gold deposits. The deepest seated level of physical inhomogeneities (lithospheric mantle and lower crust) corresponds to the ore district or several closely spaced districts. In our case, this is the Pilda–Limuri gold district, which occupies almost half of the ring structure, and the Kherpuchin district located in the northern part (Fig. 1), which has a much smaller size and, in general, composes a single body with the former district. Physical inhomogeneities of the upper–middle crust could be correlated to the ore clusters or their highest grade portions, as well as deposits proper.

In the central part of the Lower Amur metallogenic zone, the gold-bearing territory, including two closely spaced ore districts, is correlated to the low-density region in the lithospheric mantle (Fig. 3). This can be considered as the first important feature of the gold district. Thus, it should be noted that the low-density mantle zone dips to the west and southwest, and its deepest seated part is located beneath the eastern half of the LARS. This deep-seated low-density zone becomes linear, has a sublongitudinal orientation, and is traced beyond the LARS for 70 km in the northern direction. This low-density band marks the permeable zone in the mantle and deep-seated fault zone in the crust. The Albazino gold cluster is located above the eastern boundary of this low-density area. It should

again be emphasized that this low-density mantle area equally spans both the studied part of the Lower Amur metallogenic zone and territory west of it, which already has been included in the Amur metallogenic province. The data suggest that this area is characterized by the common deep structure controlled by the same magmatic processes and ore formation. This also suggests a common metallogenic specialization of its eastern and western parts, which is supported by the presence of the Albazino gold cluster in the northwestern LARS. This in turn suggests that the gold potential of the western part of the distinguished ring structure was underestimated.

The second feature of the ore district could be its saturation in the local low-density areas at depths up to 20–25 km. These areas correspond to separate intrusions of felsic composition and feeders (permeable zones), where the rocks were subjected to metasomatic alterations. The presence of such magmatic centers determined the ore generation within their limits and along periphery. It should be also noted that intrusions in the upper crust, which are reflected in the gravity field within ore districts, do not always have a granitoid composition, i.e., determine the lower gravity field. In some cases, this could be denser rocks such as diorites and gabbrodiorites, which could correspond to positive gravity anomalies and correspondingly, are marked by the low-density areas [22].

In the magnetic field, the considered area also is not defined by a single anomaly, but it is well seen that LARS and gold-bearing areas are characterized by the extremely high saturation in magnetic bodies, which are interpreted as intrusions located at different crustal levels.

Ore clusters, fields, and separate deposits are spatially correlated already with physical inhomogeneities in the upper and middle crust.

To analyze these patterns, let us consider the position of major deposits of the area relative to the density and magnetic crustal inhomogeneities. Thus, the deposit is referred to not as point, but as definite area surrounding it and corresponding to the highest grade part of the gold cluster.

The Albazino deposit is located in the vicinity of the small Upper Albazino granodiorite massif of the Lower Amur complex [7]. According to [24], it is located within the strongly eroded caldera. According to the analysis of magnetic model at depths up to 1 km, the deposit is sandwiched between weakly magnetic bodies. Beginning from a depth of 1 km, it is clearly seen that the deposit is located in the marginal part of a zone of narrow sublongitudinal magnetic bodies, which is traced southward for almost 60 km (Fig. 2b). This pattern with different variations is observed to a depth near 8 km. Below, the magnetic bodies disappear and again appear at a depth of 12 km as relatively large, equant magnetic bodies, which are arranged one after the other in the sublongitudinal direction along the considered above sublongitudinal fault. The size of these bodies is approximately 20*30 km. Thus, the Albazino deposit is located above the northern boundary of one of them. Following the accepted interpretation, these magnetic bodies could be considered as deep-seated portions of magnetic intrusions.

The deposit is located in the marginal part of the crustal low-density zone, which has a sublongitudinal orientation and length near 100 km at a width of 15–45 km. This zone is situated in the western outer part of the RS beneath the Evur volcanic edifice. The Albazino deposit is located above the boundary of this low-density area, in its northern narrow part. The longitudinal low-density zone is also distinguished in mantle, and the deposit is confined to the marginal part of this zone.

The Chulbatkan deposit. The Chulbat plagiogranite massif spatially associated with deposit is not distinguished in the magnetic field and in the magnetic model. Its low magnetic susceptibility is also emphasized in [1]. However, a large magnetic body is seen to the north of deposit at depths of 2–6 km, with deposit located above its southern boundary. We suggest that this is an unexposed intrusive massif. At a depth of 6–10 km, all anomalies of effective magnetization practically disappear. However, beginning from a depth of 12 km, a magnetic body with high effective magnetization again appears to the northeast of the deposit. This body is not correlated with known intrusive massifs, being located between the Chulbat and Dalzhin intrusions and likely represents their root portion. The deposit lies above the southern boundary of this deep-seated magnetic field.

The Chulbatkan deposit is the only deposit confined to the central part of the local low-density zone in the upper–middle crust.

The Pokrovo-Troitskoe deposit is confined to the contact of small magnetic body, which is involved in a general chain of the same NE-trending bodies almost 70 km long. These magnetic bodies are traced to a depth of 4 km and then disappear. The depth level of 5–13 km practically shows no anomalies of effective magnetization, except for some bodies of sublongitudinal orientation with low effective magnetization. A large magnetic body 25 km across appears from a depth of 15 km to the southeast of the deposit (Fig. 2d). It is traced to a depth of 20 km and the deposit is confined to its northeastern boundary. In the density model, the Pokrovo-Troitskoe deposit is confined to the marginal near-contact part of the low-density area, which in general is equant body 50 km across. The density boundary that underlies the deposit extends further eastward for approximately 100 km, leaving the limits of the ring structure.

The Oktyabr'skoe deposit is a very small deposit. Down to a depth of 2 km, the deposit is spatially associated with a group of closely spaced magnetic bodies in general extending for 30 km from the deposit to the

northeast. One of them coincides with the Malov'yunsky intrusive massif, with deposit confined to its contact [11]. With increasing depth, the pattern is generalized and a single NE-trending magnetic body is observed at a depth of 8 km, which is extended for 50 km at a width of 8–10 km. The deposit is restricted to its southeastern contact. Further to a depth of 12 km, magnetic bodies are absent in this area, and a small magnetic body was distinguished only at depth of 16 km, to the south of the deposit.

The deposit occupies a definite position in the northern marginal part of the crustal low-density zone, the southern boundary of which is correlated to the Pokrovo-Troitskoe ore field (Fig. 3).

The Agnie-Afanas'evskoe deposit. The NE-trending small magnetic bodies are observed to a depth of 1.5 km. At depths of 2–8 km, the deposit is underlain by several narrow, up to 10-km-wide sublongitudinal magnetic bodies 50-km long. This zone is traced further southward up to the Uchaminsky deposit. The Agnie-Afanas'evskoe deposit is located above the northern continuation of the zone, between narrow magnetic bodies, in the area with lowered magnetization. These magnetic bodies likely emphasize the Limurchan fault system. At a depth of 10–14 km, the effective magnetization anomalies are absent. Starting from 15 km, large NE-trending magnetic body appears to the south of the deposit (Figs. 3d, 5). The Agnie-Afanas'evskoe deposit and several gold occurrences are correlated with the northern boundary of this body. The distribution of magnetic bodies here clearly emphasizes two directions of possible faults: sublongitudinal and northeastern.

The deposit is localized in the northern marginal part of the low-density crustal area of a general NE orientation with a size of 40 x 80 km.

The Uchaminsky deposit is restricted to the same system of sublongitudinal magnetic bodies as the Agnie-Afanas'evskoe deposit, 25 km south of it. The magnetization pattern up to a depth of 15 km is similar to that of the Agnie-Afanas'evskoe deposit. Starting from a depth of 15 km, the deposit is underlain by the large magnetic body considered above. Thus, the Uchaminsky deposit, unlike many other deposits, is located directly above its center (Fig. 5). This is also the case for the Alochka, Sluchainoe, Kvartsevoe, and Valunistoe occurrences.

In the model of density distribution, the position of the deposit also slightly differs from other objects. It is localized almost above center of the low-density crustal area.

The Dyappe and Martem'yanovskoe deposits are similar in the density pattern and magnetic parameter. Down to a depth of 2–3 km, they are conjugate with weakly magnetic NE-trending body. From 4 to 12 km, the magnetic bodies in the deposit area are absent. Starting from 15 km, the magnetic body considered above when characterizing the Uchaminsky and Agnie-Afanas'evskoe deposit appears to the south and west of the deposits.

As to the density crustal inhomogeneities, both these deposits are restricted to the southeastern contact of the low-density area, which is also spatially associated with the Agnie-Afanas'evskoe and Uchaminsky deposits. The sharp boundary of the low-density area coinciding with the boundary of magnetic body suggests a NE-trending fault in this area.

The Delken deposit is located near the southern contact of the Limurchan granodiorite massif. This massif is manifested in the magnetic model as a single sublongitudinal magnetic body up to a depth of 8 km. At greater depths, magnetic bodies were not identified. Only at depth of 15–20 km to the east of the deposit, we observe the large magnetic body, which, as mentioned above, is correlated with the Agnie-Afanas'evskoe and Uchaminsky deposits. The deposit is located in the marginal part of the sublongitudinal low-density area in the crust. However, this area, unlike the above mentioned, belongs to the system of low-density bodies, which is extended in the sublongitudinal direction from the Albazino deposit.

Analysis of distribution of separate groups of gold occurrences relative to the density and magnetic crustal inhomogeneities leads to approximately the same conclusions as for deposits.

All considered objects are correlated with the marginal northern, eastern, and southern parts of the low-density mantle zone.

Thus, the correlation of known deposits (most productive part of ore clusters) with the geological structural and geophysical characteristics of the considered area allowed us to draw the following conclusions.

(1) Ore objects are clearly confined to the marginal parts of the low-density crustal areas. This means that gold mineralization is localized mainly in the marginal parts of large intrusive systems developed at depths up to 20–25 km in the crust.

(2) Based on the correlation of gold clusters and deposits with magnetic bodies, it was established that:

(a) gold clusters are confined to the marginal parts of magnetic bodies of the lowermost level located at depths greater than 12–14 km. It is clearly seen that gold deposits (except for the Uchaminsky deposit and some occurrences) usually are not correlated with the central parts of magnetic bodies at depth. Therefore, the localization of gold mineralization in the marginal parts of the intrusions of this level is an important deep-seated feature;

(b) the depth level from 8 to 12 km beneath ore clusters usually is devoid of effective magnetization anomalies. The distribution of this parameter at the given depths has a near-zero average level and a weak differentiation;

(c) deposits are correlated with magnetic bodies of the 2–8 km level. They frequently have a linear shape

and are confined to the NS- and NE-trending zones, thus determining ore-controlling faults and, hence, are important for prediction of gold mineralization. This level is also characterized by the relatively large magnetic bodies, with mineralized areas restricted to their marginal parts.

The deposits in most cases associate with magnetic bodies of the upper level (up to 2 km). Thus, it should be noted that the latter not always coincide with intrusive bodies distinguished from geological data. This may indicate both the initial low concentration of magnetic phases in these massifs and a decrease of magnetic parameters in relation with the influence of superimposed hydrothermal alterations. Thus, such geologically mapped massifs are almost always correlated with magnetic bodies, which can be interpreted as their unexposed parts, likely indicating the secondary alteration of magnetic properties of the subsurface portions of the intrusions. However, the details of magnetic survey on a scale of 1 : 50 000 and, moreover 1 : 200000, are insufficient to study the uppermost crust, and a more detailed ground magnetic survey is required.

Thus, we established that ore clusters, fields, and deposits are spatially confined to the marginal parts of deep-seated magnetic bodies interpreted as intrusive bodies. This can be important prospecting feature for the recognition of potential gold-bearing areas. Thus, as mentioned above, these magnetic bodies do not coincide or partially coincide with the low-density areas in the crust.

The next factor responsible for the distribution of gold mineralization is fault zones distinguished using geophysical parameters. Based on orientation, they are subdivided into two groups.

Of the most interest are faults of the first group, that is, the sublongitudinal zone intersecting the ring structure. As mentioned previously, this zone in the mantle is correlated with a linear low-density area. The NS-trending low-density zone of lesser extension is identified in the crust, which underlies the Evur volcanic structure and series of less contrasting low-density areas to the south. All zones of this fault, especially along the periphery of deep-seated intrusions, in our opinion, are promising to prospect for gold deposits. They could be localized both in the Jurassic sediments and in the volcanogenic rocks. It is possible that mineralization in this fault zone will be located at greater depth. It should be also noted that the possible discovery of gold deposits in the "Jurassic" portion of the ring structure, to the west of the Limurchan fault, southward of the Albazino deposit, is underestimated. We suggest that the western part of the LARS, including the Albazino gold cluster and ore districts of the Lower Amur metallogenic zone (Pilda–Limuri and Kherpuchin), are ascribed to the single ore-magmatic system, the gold potential of which was formed by the single processes of magmatism and ore formation.

The second group of linear geophysical elements has an ENE strike. In terms of direction, it corresponds to the known large fault zones passing through the area but spatially does not coincide with them.

The scheme presented above of the deep structure of LARS (Fig. 5) shows the promising areas for prospecting works. They were distinguished based on the above-considered geophysical features and could facilitate the development of prospecting works for bedrock gold in the Lower Amur metallogenic zone.

CONCLUSIONS

(1) The Limuri–Amgun ring structure has been identified in the central part of the Lower Amur metallogenic zone based on geophysical data. Its manifestation and peculiarities are caused by the high saturation in magmatic bodies of different compositions, their mutual position in the upper and middle parts of the crust, and physical inhomogeneities in the lower crust and mantle. The physical inhomogeneities typical of this structure could be traced to the asthenosphere boundary. We suggest that the formation of this structure was related to the ascent of fluids from a suprasubduction mantle wedge and melts generated in the upper part of lithospheric mantle and lower crust.

(2) The considered structure is related to the processes on the active Asian margin in the Late Cretaceous–Early Paleogene. Magmatism of this stage was mainly related to subduction. It spanned both Jurassic and Cretaceous sediments of terranes of the Sikhote Alin orogenic belt and Triassic and Jurassic sediments of the terranes of the Mongol–Okhotsk orogenic belt.

(3) The distinguished ring structure is saturated in gold objects and corresponds to the large ore-magmatic system. In this area, the gold mineralization is genetically related to the Late Cretaceous magmatic activity in a subduction setting.

(4) The revealed features of the depth structure and distribution of physical inhomogeneities in the crust provide important information for the recognition of areas promising to prospect for gold mineralization. Based on these data, areas appropriate for special and prospecting works for gold were distinguished within the Limuri–Amgun ring structure.

(5) At the modern stage of studies in the central part of the Lower Amur metallogenic zone: (a) the gold potential of the western Lower Amur metallogenic zone is underestimated; (b) the consolidation of prospecting works along periphery of deep-seated magmatic paleochambers is justified; (c) the study of the ore localization (fault tectonics, permeable zone, barriers, zones of hydrothermal alterations) in the upper part of the section requires detailed geophysical, ground geophysical, or airborne surveys with small aircraft.

The results of this work bring us closer to understanding and, respectively, explaining the high gold

potential of the central part of the Lower Amur metallogenic zone. The established features of its deep structure can be used for the recognition of new promising areas for prospecting works.

ACKNOWLEDGMENTS

We are grateful to reviewers D.L. V'yunov and V.E. Kuznetsov for thorough study of the manuscript and valuable comments that significantly improved it.

FUNDING

This work was supported by the Government of the Khabarovsk Krai for Scientific Studies (Natural and Technical Sciences) in 2022 (Agreement no. 86C/2022 of November 10, 2022). This work was made in the framework of the government-financed task of the Institute of Tectonics and Geodynamics of the Far Eastern Branch, Russian Academy of Sciences and the Geological Institute of the Russian Academy of Sciences.

CONFLICT OF INTEREST

The authors declare that they have no conflicts of interest.

REFERENCES

1. A. S. Alekseev and V. I. Starostin, "The new gold deposit in the Lower Amur Region: Chulbatkan, Khabarovsk Region," Moscow Univ. Bull. Geol. Bull. **72** (2), 126–131 (2017).
2. B. A. Andreev and I. G. Klushin, *Geological Interpretation of Gravity Anomalies* (Nedra, Leningrad, 1965) [in Russian].
3. *Geodynamics, Magmatism, and Metallogeny of East Russia*, Ed. by A. I. Khanchuk (Dal'nauka, Vladivostok, 2006), **Vol. 1** [in Russian].
4. *GIS-Atlas Interior of Russia. Far East Federal Region. Khabarovsk Krai. Map of Metallogenic Zoning by September 01, 2021.* http://atlaspacket.vsegei.ru/#a-12e28281b7771117
5. P. Yu. Gornov and G. Z. Gil'manova, "Thermal field and geothermal models of the lithosphere in the continent–ocean transition zone of northeastern Asia," Russ. Geol. Geophys. **59** (8), 1039–1048 (2018).
6. *State Geological Map of the Russian Federation. 1 : 1000000 (3rd Generation). Far East Series. Sheet N-53. Shantarskie Islands. Geologica Map. Sheet 1* (Kartfabrika VSEGEI, St. Petersburg, 2007) [in Russian].
7. *State Geological Map of the Russian Federation. 1 : 1000000 (3rd Generation). Far East Series. Sheet N-53. Shantarskie Islands: Explanatory Note* (Kartfabrika VSEGEI, St. Petersburg, 2007) [in Russian].
8. *State Geological Map of the Russian Federation. 1 : 1000000 (3rd Generation). Far East Series. Sheet M-53. Khabarovsk. Geological Map. Sheet 1* (Kartfabrika VSEGEI, St. Petersburg, 2009) [in Russian].
9. *State Geological Map of the Russian Federation. 1 : 1000000 (3rd Generation). Far East Series. Sheet M-53. Khabarovsk: Explanatory Note* (Kartfabrika VSEGEI, St. Petersburg, 2009) [in Russian].
10. *State Geological Map of the Russian Federation. 1 : 1000000 (3rd Generation). Far East Series. Sheet N-54. Nikolaevsk-on-Amur. Geological Map. Sheet 1* (Kartfabrika VSEGEI, St. Petersburg, 2016) [in Russian].
11. *State Geological Map of the Russian Federation. 1 : 1000000 (3rd Generation). Far East Series. Sheet N-54. Nikolaevsk-on-Amur: Explanatory Note* (Kartfabrika VSEGEI, St. Petersburg, 2016) [in Russian].
12. *State Geological Map of the Russian Federation. 1 : 1000000 (3rd Generation). Far East Series. Sheet M-54. Aleksandrov-Sakhalinskii. Geological Map of Pre-Quaternary Rocks. Sheet 1* (Kartfabrika VSEGEI, St.Petersburg, 2017) [in Russian].
13. *State Geological Map of the Russian Federation. 1 : 1000000 (3rd Generation). Far East Series. Sheet M-54. Aleksandrov-Sakhalinskii: Explanatory Note* (Kartfabrika VSEGEI, St. Peterburg, 2017) [in Russian].
14. A. N. Didenko, M. Yu. Nosyrev, B. F. Shevchenko, and G. Z. Gil'manova, "Thermal structure of Sikhote Alin and adjacent areas based on spectral analysis of the anomalous magnetic field," Dokl. Earth Sci. **477** (1), 1368–1372 (2017).
15. A. N. Didenko and M. Yu. Nosyrev, "Density structure of the lithosphere of the Sikhote-Alin Orogenic Belt," Dokl. Earth Sci. **492** (2), 446–450 (2020).
16. Dobretsov N.L., Koulakov I.Yu., Litasov K.D., Kukarina E.V. "An integrate model of subduction: contributions from geology, experimental petrology, and seismic tomography," Russ. Geol. Geophys. 2015 **56** (1–2), pp. 13–38.
17. N. L. Dobretsov, V. A. Simonov, I. Yu. Koulakov, and A. V. Kotlyarov, "Migration of fluids and melts in subduction zones and general aspects of thermophysical modeling in geology," Russ. Geol. Geophys. **58** (5), 571–585 (2017).
18. V. Yu. Zabrodin, O. V. Rybas, and G. Z. Gil'manova, *Fault tectonics of the continental part of the Russian Far East* (Dal'nauka, Vladivostok, 2015) [in Russian].
19. V. Yu. Zabrodin, "Structure and evolution of the Badzhal volcanoplutonic area (Far East)," Regional. Geol. Metallogen, No. 75, pp. 9–59 (2018).
20. *Complex of Spectral–Correlation Analysis of Data COSCAD 3D. Version 2018.1* (MGRI, Moscow, 2018), part 1 [in Russian].
21. V. G. Moiseenko and L. V. Eirish, *Gold Deposits of East Russia* (Dal'nauka, Vladivostok, 1996) [in Russian].
22. M. Yu. Nosyrev, "Geophysical characteristics of shallow intrusions in gold clusters of the southern Far East," *Tectonics, Deep Structure, and Metallogeny of East Asia: 11th Kosygin Readings. Proc. All-Russian Conference with International Participation, Khabarovsk, Rus-*

sia, 2021, Ed. by A. N. Didenko and Yu. F. Manilov (ITiG DVO RAN, Khabarovsk, 2021), pp. 103–105 [in Russian].

23. A. V. Petrov, D. B Yudin., and H. Syueli, "Processing and interpretation of geophysical data by the probability statistical approach with a use of COSCAD 3D Computer Technology," Vestn. KRAUNTs. Nauki o Zemle, No. 2 (16), 126–132 (2010).

24. S. I. Trushin and V. E. Kirillov, "Albazino deposit is a new economic type of gold mineralization in the Far East," Region. Geol. Metallogen. **73**, 60–66 (2018)

25. A. N. Didenko, M. Y. Nosyrev, and G. Z. Gil'manova, "A gravity-derived Moho model for the Sikhote Alin Orogenic Belt," Pure Appl. Geophys. (2021). https://doi.org/10.1007/s00024-021-02842-26

26. A. I. Khanchuk and I. V. Kemkin, "Jurassic geodynamic history of the Sikhote-Alin-Priamurye region," *Late Jurassic Margin of Laurasia: a Record of Faulting Accommodating Plate Rotation*, Ed. by T. N. Anderson (Geol. Soc. Am., Boulder, 2015), pp. 509–525.

Translated by M. Bogina

Recommended for publishing by V.B. Kaplun